Chemical Science

Accepted Manuscript

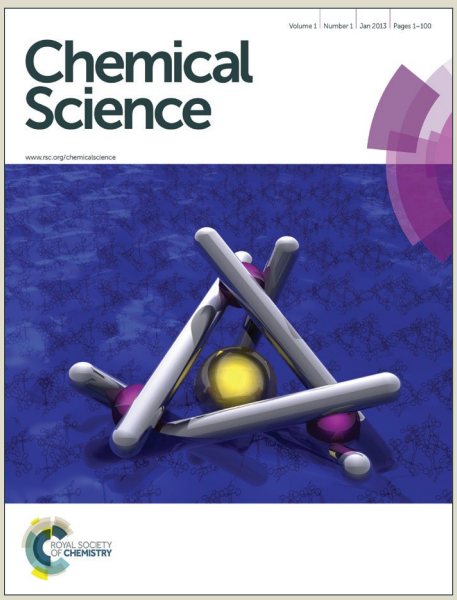

ROYAL SOCIETY OF CHEMISTRY

www.rsc.org/chemicalscience

Chemical Science

EDGE ARTICLE

Supercoiled fibres of self-sorted donor-acceptor stacks: a turn-off/turn-on platform for sensing volatile aromatic compounds

85897Received 00th January 20xx,
Accepted 00th January 20xx

DOI: 10.1039/x0xx00000x

www.rsc.org/

Anjamkudy Sandeep,[a] Vakayil K. Praveen,[a] Kalathil K. Kartha,[a] Venugopal Karunakaran[a,b] and Ayyappanpillai Ajayaghosh*[a,b]

To ensure the comfortable survival of living organisms, detection of different life threatening volatile organic compounds (VOCs) such as biological metabolites and carcinogenic molecules are of prime importance. Herein, we report the use of supercoiled supramolecular polymeric fibers of self-sorted donor-acceptor molecules as "turn-off-turn-on" fluorescent sensors for the detection of carcinogenic VOCs. For this purpose, a C_3-symmetrical donor molecule based on oligo(*p*-phenylenevinylene), C_3OPV and a perylene bisimide based acceptor molecule, C_3PBI have been synthesized. When these two molecules were mixed together in toluene, in contrast to the usual charge transfer (CT) stacking, supramolecular fibers of self-sorted stacks were formed at the molecular level, primarily driven by their distinct self-assembly pathways. However, CT interaction at macroscopic level allows these fibers to bundle together to form supercoiled ropes. Interfacial photoinduced electron transfer (PET) process from the donor to the acceptor fibers leads to the initial fluorescence quenching, which could be modulated by exposure to strong donor or acceptor type VOCs to regenerate the respective fluorescence of the individual molecular stacks. Thus, strong donors could regenerate the green fluorescence of C_3OPV stacks and strong acceptors could reactivate the red fluorescence of C_3PBI stacks. These supercoiled supramolecular ropes of self-sorted donor-acceptor stacks provide a simple tool for the detection of donor- or acceptor-type VOCs of biological relevance, by a "turn-off/turn-on" fluorescence mechanism as demonstrated with *o*-toluidine, which is reported as a lung cancer marker.

Introduction

Early detection of deadly diseases such as cancer can save the life of millions of people across the globe and hence a prime concern of scientists and clinicians. At the onset of certain diseases, the metabolism of the human body changes to produce several volatile organic compounds (VOCs) in small quantities, some of which can be designated as disease markers.[1] Detection of cancer markers and carcinogenic VOCs such as *o*-toluidine, aromatic amines, nitro aromatics etc. are important since tobacco smoke contains a large number of them, which are known to cause bladder cancer.[2a] *o*-Toluidine has also been detected in the exhaled air of lung cancer patients.[2b] Similarly, detection of electron deficient molecules such as nitroaromatics are important since they are not only considered as explosives but also toxic to living organisms by contaminating air and water.[3]

Considering the social relevance of the detection of carcinogenic VOCs, intense research is needed for further development in this area. These considerations have prompted us to explore the potential of fluorescent donor-acceptor assemblies designed based on the principles of nanoarchitectonics[4] for sensing of volatile analytes. A number of reports are available for the sensing of VOCs such as aromatic amines[5] and nitroaromatics[3,6,7] that generally cause fluorescence quenching of a probe. In this context, self-sorted supramolecular assemblies[8-10] is an ideal platform for the sensing of VOCs. We have earlier shown that fluorescent π-gelators are powerful tools for the attogram level sensing of trinitrotoluene (TNT) on a contact mode[7a] and thought the

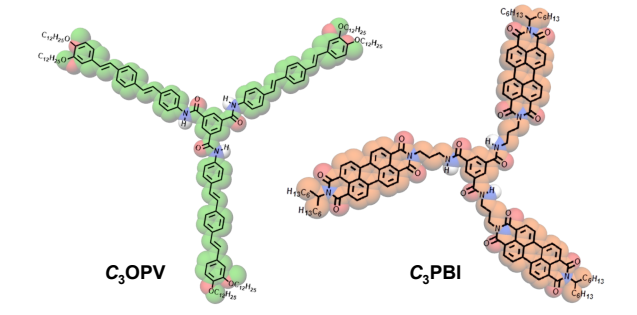

Fig. 1 Chemical structures and molecular models (shown in shadow) of C_3**OPV** and C_3**PBI**.

[a] *Photosciences and Photonics Section, Chemical Sciences and Technology Division, CSIR-National Institute for Interdisciplinary Science and Technology (CSIR-NIIST), Thiruvananthapuram 695 019, India. Email: ajayaghosh@niist.res.in*
[b] *Academy of Scientific and Innovative Research (AcSIR), CSIR-NIIST Campus, Thiruvananthapuram 695 019, India.*

†Electronic Supplementary Information (ESI) available: [Materials and methods, synthesis procedures and characterization data of compounds, details about the isodesmic and nucleation-elongation models and additional figures]. See DOI: 10.1039/x0xx00000x

immense scope for expanding this idea to the sensing of VOCs of metabolic origin, if the principles of molecular self-assembly and self-sorting are combined.

Usually, when donor and acceptor monomers are mixed, CT induced supramolecular polymers are formed.[11] A supramolecular control on the polymerization is difficult in such cases.[12] However, suitably functionalized π-systems[10] such as oligo(thiophenes) (OTs), oligo(*p*-phenylenevinylene) (OPVs) and perylene bisimides (PBIs) are known to form self-sorted supramolecular polymeric stacks when mixed, in which the emission is quenched due to photoinduced electron transfer (PET) from the electron rich OTs or OPVs to the electron deficient PBIs.[10a,b] Recently, we have reported the formation of self-sorted supramolecular assemblies of thienylenevinylenes and PBIs that form coaxial fibres[10d] through the week interfacial charge transfer interaction.[13] Based on these findings, we hypothesized that, suitably designed C_3-symmetrical systems of OPVs and PBIs may form supramolecular polymers of self-sorted donor and acceptor fibres with quenched fluorescence. In such a case, the weak interfacial donor-acceptor interaction in supercoiled fibres at supramolecular level can be perturbed by exposure to a strong donor or acceptor molecular vapours, which may results in a "turn-on" fluorescence with distinct colour variation. As a proof-of-concept to this hypothesis, we illustrate that a combination of a C_3-symmetrical OPV, ***C*₃OPV** and a C_3-symmetrical PBI, ***C*₃PBI**, (Fig. 1) form supercoiled fibers of self-sorted donor-acceptor stacks, which resulted in a "turn-off/turn-on" fluorescence sensor for the detection of different aromatic VOCs.

Results and discussion

Synthesis of the ***C*₃OPV** and ***C*₃PBI** was accomplished as shown in Scheme S1† and S2†, respectively and were characterised using FT-IR, ^{1}H and ^{13}C NMR spectroscopies and MALDI-TOF mass spectrometry. Having these molecules in the pure form, our first objective was to get a clear idea of the mechanistic pathway of the individual assembly of ***C*₃OPV** and ***C*₃PBI**. Detailed UV/Vis absorption studies revealed that these molecules self-assemble in toluene at a concentration range of 10^{-4} to 10^{-5} M (Fig. S1†). Further understanding of the self-assembly mechanism was possible from the temperature-dependent absorption studies. For this purpose, the change in the absorption shoulder band at 425 nm of a hot toluene solution of (1 x 10^{-4} M) ***C*₃OPV** was monitored as a function of temperature with a cooling rate of 1 K min^{-1} (Fig. S1b†). No hysteresis was observed when the solution was heated again

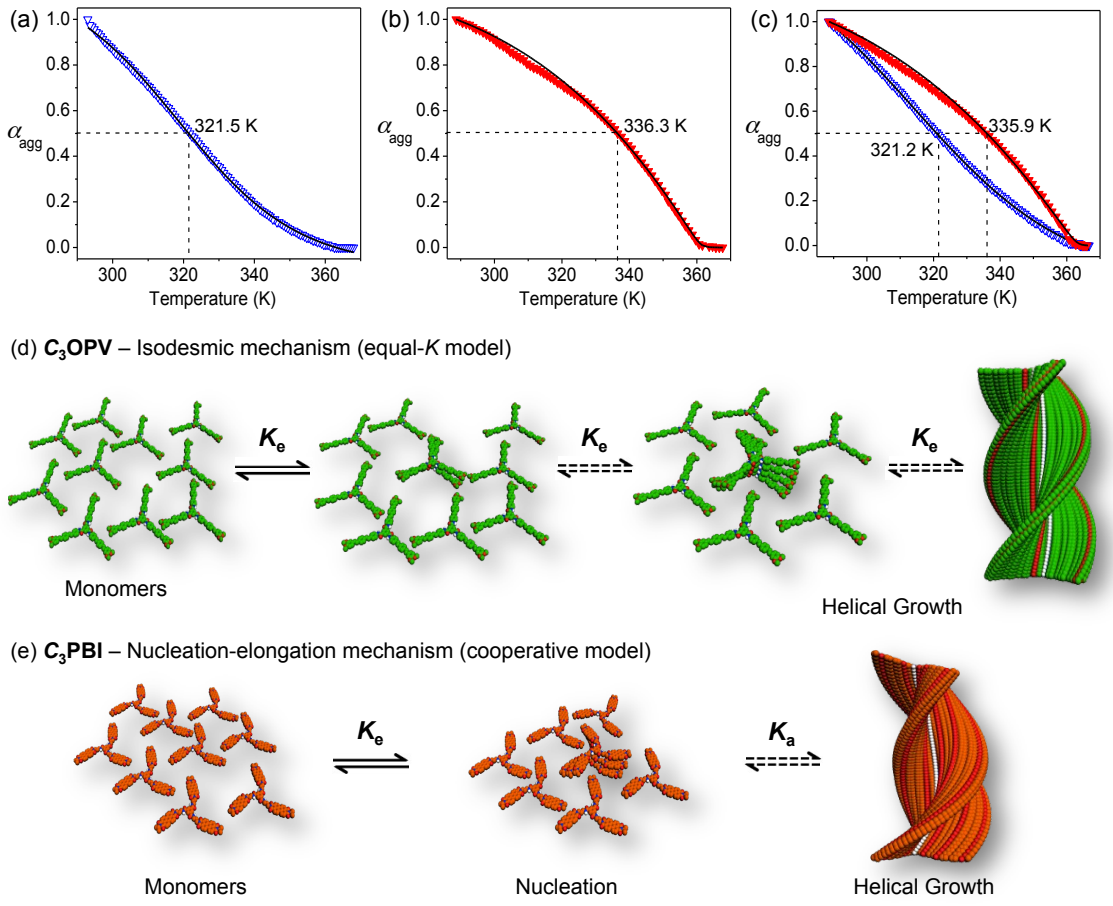

Fig. 2 Plot of fraction of aggregates (α_{agg}) against temperature for (a) ***C*₃OPV** and (b) ***C*₃PBI** individual assemblies and (c) for ***C*₃OPV** and ***C*₃PBI** in the 1:1 mixture in toluene (1 × 10^{-4} M). ***C*₃OPV** (Δ), ***C*₃PBI** (▼) and fit (—). Absorbance was monitored at 425 and 527 nm for ***C*₃OPV** and ***C*₃PBI**, respectively with a rate of cooling of 1 K min^{-1}. Schematic illustration of the self-assembly pathway of (d) ***C*₃OPV** (e) ***C*₃PBI**. K_e is the association constant and K_a is the activation constant expressing the degree of cooperativity.

to the monomeric state, indicating that the self-assembly process is reversible. It is clear from the plot of the fraction of aggregates (α_{agg}) versus temperature that the molecule forms assembly through an isodesmic pathway (equal-*K* model) as indicated by the broad melting curve, which could be fitted with the standard isodesmic model (Fig. 2a).[14] This observation is quite surprising, especially from the fact that most of the C_3-symmetrical benzene trisamide derivatives are known to self-assemble through a cooperative nucleation-elongation mechanism.[15] Based on this observation, we concluded that the isodesmic self-assembly of ***C*$_3$OPV** (Fig. 2d) presumably is governed by π-π stacking of the OPV moieties and the contribution from directional intermolecular H-bonding may be weak due to the presence of sterically demanding aromatic core and the six alkyl chains at the periphery.[15,16] The thermodynamic parameters are calculated by applying the isodesmic model and are summarized in Table 1. The melting transition temperature (T_m, temperature at which α_{agg} = 0.50) of the assembly is found as 321.5 K (Fig. 2a) with an enthalpy value of -85.1 kJmol^{-1} and an association constant of 4.7 × 10^4 M^{-1}.

To probe the self-assembly pathway of ***C*$_3$PBI**, the absorption changes at 527 nm was monitored as a function of temperature with a cooling rate of 1 K min^{-1} (Fig. S1d†). The plot of α_{agg} with temperature showed a non-sigmoidal transition, characteristic of a cooperative pathway, which could be fitted with the nucleation-elongation model (Fig. 2b and 2e).[14c,15a,17-19] By applying this model, the elongation temperature (T_e) is determined as 360.5 K and the enthalpy release upon elongation (H_e) is calculated as -27.4 kJ mol^{-1}. The high degree of cooperativity (K_a) is inferred from the small value of the equilibrium constant (10^{-6}) for the nucleation step.

After having an idea of the individual assembly mechanism of ***C*$_3$OPV** and ***C*$_3$PBI** in toluene, we studied the effect of mixing these molecules at a 1:1 ratio by monitoring the changes in the absorption spectrum under identical experimental conditions. The resultant spectrum of the mixture in toluene (1 × 10^{-4} M) is found to be a sum of the absorption spectra of the individual constituents (Fig. S2†). Furthermore, the absence of a CT band in the absorption spectrum excludes the possibility of a molecular level donor-acceptor interaction. The mixture was cooled down slowly with a rate of 1 K min^{-1}. Variable temperature absorption spectral change of the mixture monitored at 425 and 527 nm exhibited the melting of the individual aggregates without much variation from their respective melting transition curves as observed in the individual assemblies (Fig. 2c and S3†). The transition curves obtained from the plot of α_{agg} versus temperature could be fitted with isodesmic model and nucleation-elongation model for ***C*$_3$OPV** and ***C*$_3$PBI**, respectively (Fig. 2c). The thermodynamic parameters calculated for the mixture from the fits are in good agreement with that of the individual assemblies. The melting transition temperature, T_m, of ***C*$_3$OPV** in the mixture is 321.2 K, which is close to that of the ***C*$_3$OPV** alone (321.5 K). Similarly, T_m of the ***C*$_3$PBI** assembly in the mixture is 335.9 K, which matches to that observed for the individual assembly of ***C*$_3$PBI** (336.3 K) (Fig. 2). The other thermodynamic parameters such as enthalpy and entropy changes of the molecules in the mixture also match with that of the individual molecular assemblies (Table 1 and 2). These results imply that both ***C*$_3$OPV** and ***C*$_3$PBI** form self-sorted stacks when they are mixed.

Other important parameters in support for the formation of self-sorted assembly are the association constant (K_e) in the case of ***C*$_3$OPV** and the degree of cooperativity (K_a) in the case of ***C*$_3$PBI** (Table 1 and 2). The association constant for the addition of individual monomer to the growing assembly of ***C*$_3$OPV** in the mixture is 3.7 × 10^4 M^{-1}, which almost matches with the value for the individual assembly of ***C*$_3$OPV** (4.7 × 10^4 M^{-1}). For the cooperative self-assembly of ***C*$_3$PBI**, the degree of cooperativity is in the range of 10^{-6}, similar to that of the individual assembly.

Table 1. Thermodynamic parameters for the self-assembly of ***C*$_3$OPV** obtained using the isodesmic model.

***C*$_3$OPV**	*C* (mM)	*ΔH* (kJ mol^{-1})	*ΔS* (J mol^{-1} K^{-1})	T_m (K)	K_e (10^4 M^{-1})	DP_N
Alone	0.1	-85.1	-194.5	321.5	4.7	2.7
In mixture	0.1	-73.6	-158.0	321.2	3.7	2.5

C the concentration, *ΔH* the change in enthalpy, *ΔS* the change in entropy, T_m the melting transition temperature, K_e the association constant and DP_N the degree of polymerization.

Table 2. Thermodynamic parameters for the self-assembly of ***C*$_3$PBI** obtained using the nucleation elongation model.

***C*$_3$PBI**	*C* (mM)	ΔH_e (kJ mol^{-1})	ΔS_e (J mol^{-1} K^{-1})	T_m (K)	T_e (K)	K_a
Alone	0.1	-27.4	-140.9	336.3	360.5	10^{-6}
In mixture	0.1	-27.5	-132.6	335.9	362.4	10^{-6}

C the concentration, ΔH_e and ΔS_e, respectively the change in enthalpy and entropy during elongation process, T_m the melting transition temperature, T_e the elongation temperature and K_a the degree of cooperativity.

Atomic force microscopic (AFM) images of ***C*$_3$OPV** drop cast from 1×10^{-4} M toluene solution on a freshly cleaved mica surface revealed the formation of micrometer long helical fibres of diameter 200-250 nm (Fig. 3a). ***C*$_3$PBI** also displayed the formation of helical fibres with diameter varying from 100-150 nm and length extended to several micrometres (Fig. 3b). For the 1:1 mixed assembly, the fibre-like morphology is retained, however, the formation of super coiled helical ropes with increased diameter (400-500 nm) is observed (Fig. 3c). The scanning electron microscopy (SEM) images also support the formation of helical fibres and supercoiled ropes (Fig. 3d-f). These observations are in analogy to the previous reports on the self-assembly of C_3-symmetrical *N*,*N*',*N*''-trialkyl benzene-1,3,5-tricarboxamide in which the amide functionality is involved in a three-fold helical array of intermolecular hydrogen bonding.[20] From the mechanistic studies and the

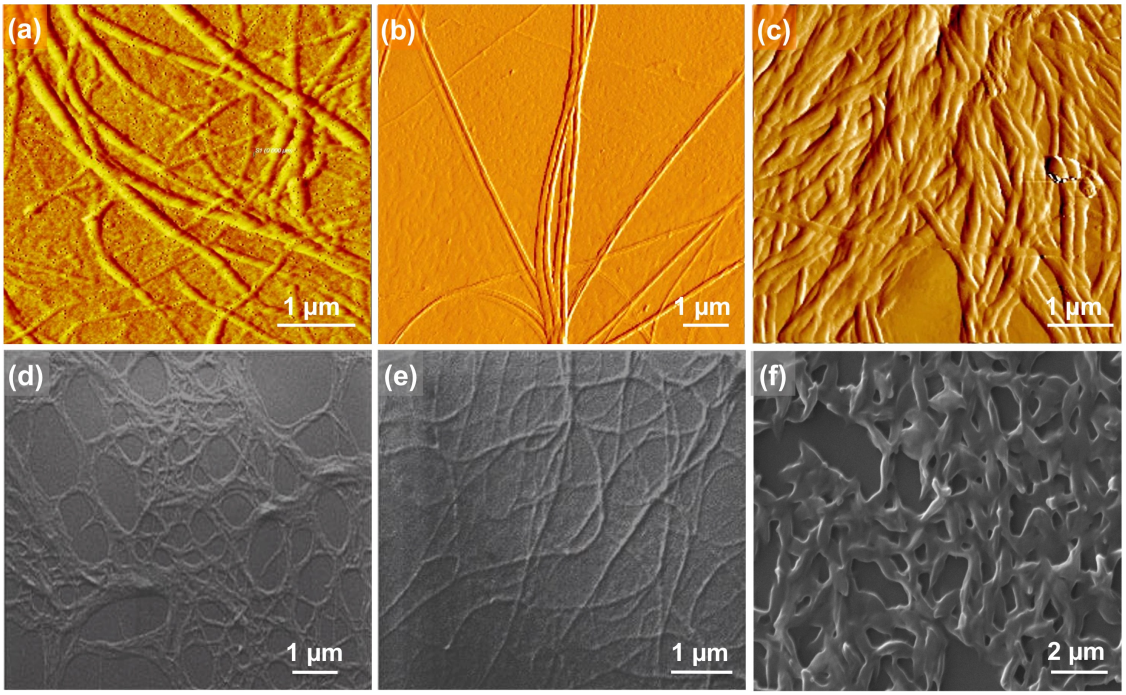

Fig. 3 AFM (a), (b) (c) and SEM (d), (e), (f) images of ***C*$_3$OPV**, ***C*$_3$PBI**, 1:1 mixture, respectively.

morphological features, it is inferred that the self-sorted donor and acceptor fibres are formed initially which enter into weak interfacial charge transfer interaction at the supramolecular level resulting in supercoiled ropes.[10d,13] The absorption spectra of a 1:1 mixture of ***C*$_3$OPV** and ***C*$_3$PBI** in the solution (toluene, 1×10^{-4} M, Fig. S2†) and film states (Fig. 4a) did not show any CT band, indicating the absence of a molecular level donor-acceptor interaction. However, significant quenching of the individual emission of ***C*$_3$OPV** and ***C*$_3$PBI** was observed in the solution and the film states (Fig. S4† and 4b). These observations could be ascribed to a possible PET from the donor OPV to the acceptor PBI.

The PET process between ***C*$_3$OPV** and ***C*$_3$PBI** was investigated using femtosecond pump-probe spectroscopy. When a solution containing 1:1 mixture of ***C*$_3$OPV** and ***C*$_3$PBI** was excited at 380 nm where mainly ***C*$_3$OPV** absorbs, transient absorption spectra showed the formation of radical anion of ***C*$_3$PBI** absorbing broadly around 630 nm with decay time of around 728 ps (Fig. 5a), which indicates PET from the OPV to the PBI.[21] The feasibility of PET between these molecules is further established by photoelectron yield spectroscopic studies (Fig. S5†). From the value of HOMO and the optical band gap (E_g) obtained from the film state absorption spectrum (Fig. S6†), LUMO of both ***C*$_3$OPV** and ***C*$_3$PBI** were calculated. ***C*$_3$PBI** showed a slightly deeper LUMO (-4.20 eV) when compared to that of ***C*$_3$OPV** (-3.50 eV) (Fig. 5b). Since ***C*$_3$PBI** is an electron accepting molecule when compared to ***C*$_3$OPV**, the HOMO level of the former is lower than that of ***C*$_3$OPV** (Fig. 5b). Therefore, upon photoexcitation, electrons are transferred from ***C*$_3$OPV** to ***C*$_3$PBI** leading to the quenching of the emission.

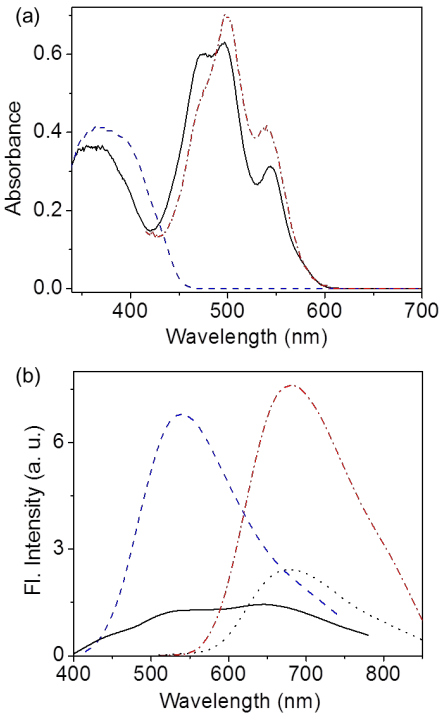

Fig. 4 (a) Absorption spectra of ***C*$_3$OPV** (---), ***C*$_3$PBI** (-•-), and 1:1 mixture of ***C*$_3$OPV** and ***C*$_3$PBI** (—) in the film state. (b) Emission spectra of ***C*$_3$OPV** (---) λ_{ex} = 375 nm, ***C*$_3$PBI** (-•-) λ_{ex} = 500 nm, and 1:1 mixture of ***C*$_3$OPV** and ***C*$_3$PBI** (—)λ_{ex} = 375 nm and (····) λ_{ex} = 500 nm in the film state.

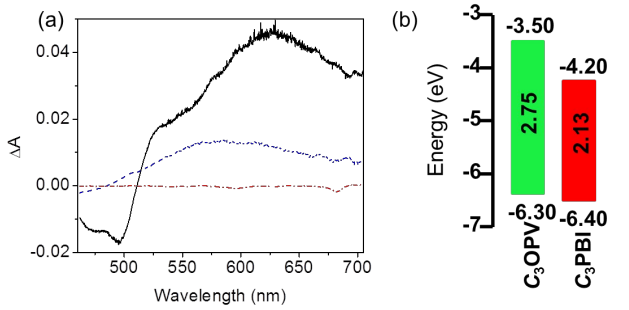

Fig. 5 (a) Transient absorption spectra of C_3**OPV** (---), C_3**PBI** (-•-) and 1:1 mixture (—) in toluene (1×10^{-4} M) recorded at 1.9 ps, λ_{ex} = 380 nm. (b) The energy level diagram for C_3**OPV** and C_3**PBI**.

Since OPVs are known to interact with electron deficient aromatic nitro compounds[3e,7a] and PBIs with electron rich aromatic amines,[5a-c,22] we thought that the quenched emission of the supercoiled C_3**OPV** and C_3**PBI** fibres could be "turned on" when comes in contact with a better donor or an acceptor molecule. In order to prove this hypothesis, a toluene solution of a 1:1 mixture of C_3**OPV** and C_3**PBI** (20 µL of 10^{-3} M) was drop cast on glass substrates and exposed to various analytes. The film that was exposed to aromatic amines such as *o*-toluidine displayed a greenish-yellow emission (Fig. 6a and 6c). Comparison of the absorption spectrum of C_3**OPV** and the excitation spectrum obtained upon monitoring the emission at 540 nm in the 1:1 mixture of C_3**OPV** and C_3**PBI** revealed that the emission originates from C_3**OPV** molecule in the mixture (Fig. S7†). On the other hand, a red emission was obtained when the film was exposed to nitrobenzene vapours (Fig. 6b and 6c). Excitation spectrum of the 1:1 mixture when monitored at 650 nm showed a resemblance to the absorption spectrum of C_3**PBI** individual assembly (Fig. S8†), which proves that the red emission is from the self-assembled C_3**PBI** molecule. Similar experiment was conducted for other aromatic amines such as 2-aminophenol, aniline, *m*-toluidine, etc. and nitroaromatics such as TNT, dinitrotoluene (DNT), *o*-nitrotoluene, etc. and the results are summarized in Fig. 7.

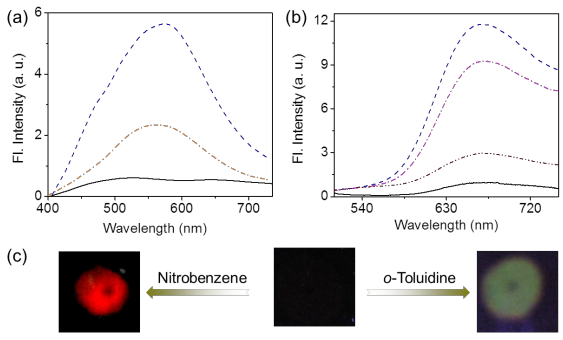

Fig. 6 The emission spectra of a 1:1 mixture of C_3**OPV** and C_3**PBI** films before and after exposing to vapours of different (a) aromatic amines [(---) o-toluidine, (-•-) aniline and (—) blank)] λ_{ex} = 375 nm and (b) nitroaromatics [(---) nitrobenzene, (-•-) 2-nitrotoluene, (-••-) 2,4-dinitrotoluene and (—) blank] λ_{ex} = 500 nm. (c) Photographs showing the fluorescence of the 1:1 mixture of C_3**OPV** and C_3**PBI** films before and after exposure to different volatile aromatic compounds.

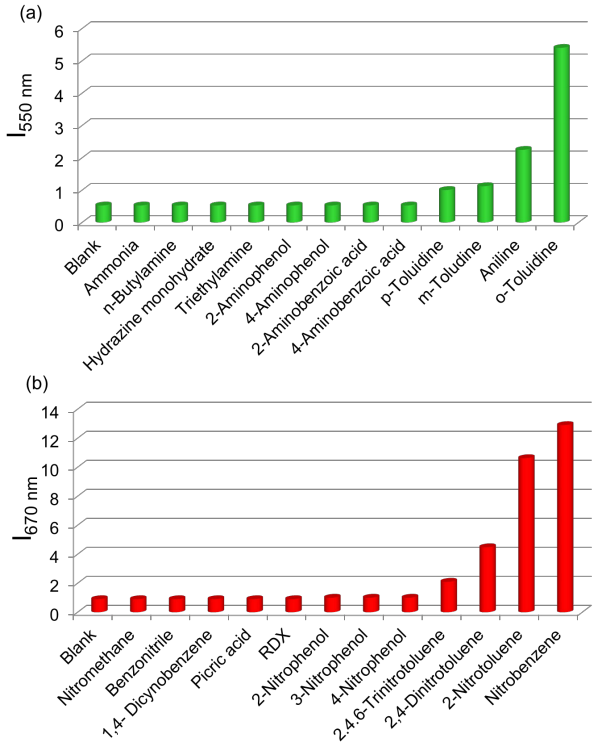

Fig. 7 Selectivity plots for the vapour phase detection of different volatile (a) amines and (b) nitro compounds using films prepared from a 1:1 mixture of C_3**OPV** and C_3**PBI**. The emission of C_3**OPV** is monitored at 550 nm (λ_{ex} = 375 nm) for aromatic amines exposed film and that of C_3**PBI** is monitored at 670 nm (λ_{ex} = 500 nm) in the case of nitro compounds exposed films. In all these studies films were exposed to VOCs for 2 min.

The observed "turn-on" emission of the mixed 1:1 C_3**OPV** and C_3**PBI** films in presence of analytes is explained as follows. Electron rich aromatic amines facilitate strong CT interaction with the electron deficient C_3**PBI** fibres, which in turn prevent the weak interfacial PET from the C_3**OPV** fibres to C_3**PBI** fibres, thus activating the C_3**OPV** emission upon excitation at 375 nm. Emission intensity revival monitored at 550 nm with time is found to depend upon the electron donating ability of the amines used (Fig. 8a). For the first 120 seconds of exposure, around 5-fold increase in the emission intensity for *o*-toluidine is observed, while only a 2-fold increase is noticed for aniline. The inductive effect of the electron donating methyl group in *o*-toluidine makes it a better donor than aniline. The inductive effect decreases in the case of *m*-toluidine as the methyl group is far from the amino group. Not only the electron donating ability of different amines but also the vapour pressure of the different amines plays an important role to the selective detection of *o*-toluidine. The vapour pressure of *o*-toluidine at 25 °C is around 200 Pa and that of aniline and *m*-toluidine is around 89 and 17 Pa, respectively. This high value of vapour pressure for *o*-toluidine and the electron donating positive inductive effect of methyl group make it fast responsive upon interaction with the film of the mixed assembly.

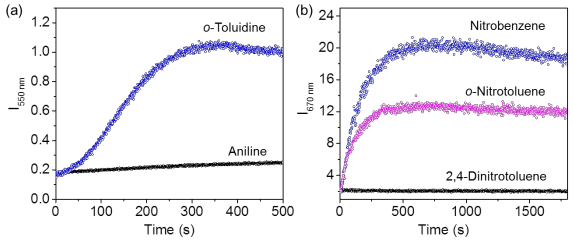

Fig. 8 Plots of emission intensity (a) at 550 nm (λ_{ex} = 375 nm) and (b) at 670 nm (λ_{ex} = 500 nm) as a function of time after exposing a film prepared from 1:1 mixture of ***C*$_3$OPV** and ***C*$_3$PBI** to the vapours of aromatic amines and nitroaromatics, respectively.

When vapours of nitroaromatic compounds such as nitrobenzene and nitrotoluene are exposed to the supercoiled fibres of ***C*$_3$OPV** and ***C*$_3$PBI**, a red emission was observed. Electron deficient nitroaromatics can have strong CT interaction with electron rich ***C*$_3$OPV** fibres thereby inhibiting the weak interfacial PET from ***C*$_3$OPV** fibres to ***C*$_3$PBI** fibres upon excitation of the later at 500 nm. Hence the interaction between the ***C*$_3$OPV** and ***C*$_3$PBI** stacks becomes weaker, thereby activating the ***C*$_3$PBI** emission by favouring more energetically feasible PET from ***C*$_3$OPV** to the electron accepting nitroaromatic compounds. In this case also, the sensitivity depends upon both the electron accepting ability and the vapour pressure of the nitro compounds. This is evident from the plot of the emission intensity monitored at 670 nm with time of exposure (Fig. 8b). It is observed that for the first one minute of exposure, nitrobenzene and 2-nitrotoluene showed almost equal amount of emission recovery. However, upon extended exposure, nitrobenzene gave more emission revival than the nitrotoluene because of its high vapour pressure (20 Pa) and electron accepting ability. When compared to nitrobenzene, the presence of electron donating methyl group reduces the electron accepting ability of *o*-nitrotoluene. At the same time, molecules such as DNT and TNT, which are more electron deficient than nitrobenzene showed less response with the film. This observation is explained on the basis of the difference in vapour pressure of these nitroaromatics. The vapour pressure of TNT and DNT are 0.0165 and 0.0079 Pa, respectively, which is much less than the vapour pressure of nitrobenzene (20 Pa) and 2-nitrotoluene (38 Pa).

The overall processes in the sensing of VOCs by the supercoiled self-stack of ***C*$_3$OPV** and ***C*$_3$PBI** are schematically shown in Fig. 9. C_3 symmetrical OPV and PBI prefer to form columnar helical assemblies of self-sorted stacks. The ***C*$_3$OPV** stacks (green) and the ***C*$_3$PBI** stacks (red), due to weak interfacial CT interaction, bundles to form supercoiled fibres (black) in which the fluorescence is quenched by PET between the donor-acceptor self-sorted fibres. The PET process is subsequently perturbed by exposing the fibres to strong donor or acceptor molecules, resulting in respective fluorescence signals of the ***C*$_3$OPV** or ***C*$_3$PBI**.

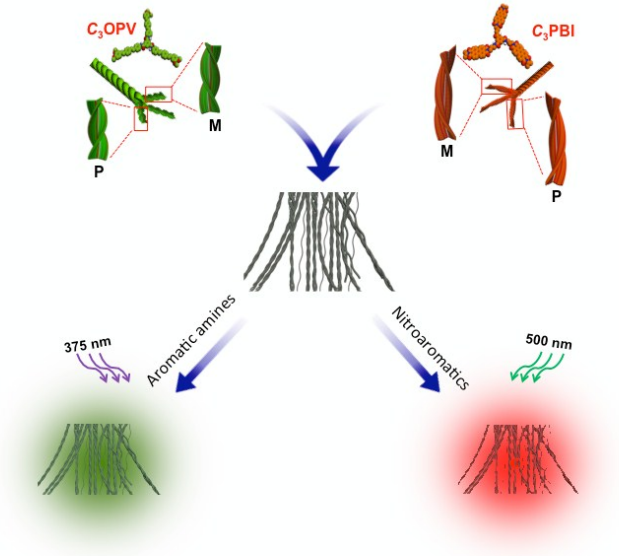

Fig. 9 Schematic illustration of fluorescence 'turn-off/turn-on' mechanism of the self-sorted fibers of 1:1 mixture of ***C*$_3$OPV** and ***C*$_3$PBI** on exposing to different VOCs.

Conclusions

By taking advantage of self-sorting at molecular level and electronic interaction at macroscopic level, we could design nonfluorescent supercoiled fibres of ***C*$_3$OPV** and ***C*$_3$PBI** molecules. The self-sorting is facilitated by the difference in the self-assembly pathway of the individual molecules wherein ***C*$_3$OPV** followed an isodesmic model and ***C*$_3$PBI** preferred a cooperative mechanism. Interfacial PET between the self-sorted fibres resulted in the quenching of the initial fluorescence of the molecules, which could be perturbed by exposure to VOCs, especially electron rich compounds such as aromatic amines and electron deficient compounds such as nitroaromatics. Thus, the green emission of ***C*$_3$OPV** appeared when exposed to *o*-toluidine and the red emission of ***C*$_3$PBI** by exposing the film to nitroaromatic vapours. Extend of emission revival depends on the electron donating ability of aromatic amines and the electron withdrawing ability of nitro aromatics in addition to the vapour pressure of the molecules. The fluorescence "turn-off-turn-on" features of the supercoiled supramolecular fibers of the self-sorted donor-acceptor system described here has the ability to detect *o*-toluidine of metabolic origin which is a known lung cancer marker.

Acknowledgments

We thank the Council of Scientific and Industrial Research (CSIR 12 FYP M2D-CSC-0134), Government of India for financial support. A.A. is grateful to the Department of Science and Technology (DST), Government of India, for a J. C. Bose Fellowship. A.S. and K.K. are thankful to CSIR, Government of India for research fellowships. V.K.P. thanks DST, Government of India for a Young Scientist Fellowship. Authors gratefully acknowledge Dr. S. Seki and Dr. A. Gopal, Osaka University,

Japan for photoelectron yield spectroscopy analyses and Ms. M. V. Chinju Govind and Mr. J. S. Kiran CSIR-NIIST, for the femtosecond pump-probe spectroscopy measurements and the artworks, respectively.

Notes and references

1 (*a*) B. Buszewski, M. Kęsy, T. Ligor and A. Amann, *Biomed. Chromatogr.*, 2007, **21**, 553–566; (*b*) A. W. Boots, J. J. B. N. van Berkel, J. W. Dallinga, A. Smolinska, E. F. Wouters and F. J. van Schooten, *J. Breath Res.*, 2012, **6**, 027108; (*c*) Y. Y. Broza and H. Haick, *Nanomedicine*, 2013, **8**, 785–806.

2 (*a*) K. Riedel, G. Scherer, J. Engl, H.-W. Hagedorn and A. R. Tricker, *J. Anal. Toxicol.*, 2006, **30**, 187–195; (*b*) G. Preti, J. N. Labows, J. G. Kostelc, S. Aldinger and R. Daniele, *J. Chromatogr. B: Biomed. Sci. Appl.*, 1988, **432**, 1–11.

3 (*a*) T. M. Swager and J. H. Wosnick, *MRS Bulletin*, 2002, **27**, 446–450; (*b*) S. J. Toal and W. C. Trogler, *J. Mater. Chem.*, 2006, **16**, 2871–2883; (*c*) K. Sakakibara, J. P. Hill and K. Ariga, *Small*, 2011, **7**, 1288–1308; (*d*) Z. Hu, B. J. Deibert and J. Li, *Chem. Soc. Rev.*, 2014, **43**, 5815–5840; (*e*) K. K. Kartha, A. Sandeep, V. K. Praveen and A. Ajayaghosh, *Chem. Rec.*, 2015, **15**, 252–265; (*f*) S. Shanmugaraju and P. S. Mukherjee, *Chem. –Eur. J.*, 2015, **21**, 6656–6666.

4 Nanoarchitectonics deal with interaction and organisation of nanoscale structures that cause emergence of new functionality, for details see: (*a*) S. Ishihara, J. Labuta, W. Van Rossom, D. Ishikawa, K. Minami, J. P. Hill and K. Ariga, *Phys. Chem. Chem. Phys.*, 2014, **16**, 9713–9746; (*b*) K. Ariga, Q. Ji, W. Nakanishi, J. P. Hill and M. Aono, *Mater. Horiz.*, 2015, **2**, 406–413; (*c*) M. Aono and K. Ariga, *Adv. Mater.*, 2016, **28**, 989–992; (*d*) K. Ariga, J. Li, J. Fei, Q. Ji and J. P. Hill, *Adv. Mater.*, 2016, **28**, 1251–1286.

5 (*a*) Y. Che, X. Yang, S. Loser and L. Zang, *Nano Lett.*, 2008, **8**, 2219–2223; (*b*) Y. Liu, K.-R. Wang, D.-S. Guo and B.-P. Jiang, *Adv. Funct. Mater.*, 2009, **19**, 2230–2235; (*c*) H. Peng, L. Ding, T. Liu, X. Chen, L. Li, S. Yin and Y. Fang, *Chem. –Asian J.*, 2012, **7**, 1576–1582.; (*d*) J. Kumpf, J. Freudenberg, S. T. Schwaebel and U. H. F. Bunz, *Macromolecules*, 2014, **47**, 2569–2573; (*e*) S. Rochat and T. M. Swager, *Angew. Chem., Int. Ed.*, 2014, **53**, 9792–9796; (*f*) A. Mallick, B. Garai, M. A. Addicoat, P. S. Petkov, T. Heine and R. Banerjee, *Chem. Sci.*, 2015, **6**, 1420–1425.

6 (*a*) A. Rose, Z. Zhu, C. F. Madigan, T. M. Swager and V. Bulović, *Nature*, 2005, **434**, 876–879; (*b*) Y. Che, D. E. Gross, H. Huang, D. Yang, X. Yang, E. Discekici, Z. Xue, H. Zhao, J. S. Moore and L. Zang, *J. Am. Chem. Soc.*, 2012, **134**, 4978–4982; (*c*) W. Zhu, W. Li, C. Wang, J. Cui, H. Yang, Y. Jiang and G. Li, *Chem. Sci.*, 2013, **4**, 3583–3590; (*d*) K. K. Kartha, A. Sandeep, V. C. Nair, M. Takeuchi and A. Ajayaghosh, *Phys. Chem. Chem. Phys.*, 2014, **16**, 18896–18901.

7 (*a*) K. K. Kartha, S. S. Babu, S. Srinivasan and A. Ajayaghosh, *J. Am. Chem. Soc.*, 2012, **134**, 4834−4841; (*b*) V. Bhalla, H. Arora, H. Singh and M. Kumar, *Dalton Trans.*, 2013, **42**, 969–997; (*c*) G. Hong, J. Sun, C. Qian, P. Xue, P. Gong, Z. Zhang and R. Lu, *J. Mater. Chem. C*, 2015, **3**, 2371–2379.

8 (*a*) M. M. Safont-Sempere, G. Fernández and F. Würthner, *Chem. Rev.*, 2011, **111**, 5784–5814; (*b*) K. Osowska and O. Miljanić, *Synlett*, 2011, 1643–1648; (*c*) C. Rest, M. Mayoral and G. Fernández, *Int. J. Mol. Sci.*, 2013, **14**, 1541–1565.

9 (*a*) J. R. Moffat and D. K. Smith, *Chem. Commun.*, 2009, 316–318; (*b*) A. Pal, P. Besenius and R. P. Sijbesma, *J. Am. Chem. Soc.*, 2011, **133**, 12987–12989; (*c*) K. L. Morris, L. Chen, J. Raeburn, O. R. Sellick, P. Cotanda, A. Paul, P. C. Griffiths, S. M. King, R. K. O. R. Reilly, L. C. Serpell and D. J. Adams, *Nat. Commun.*, 2013, **4**, 1480; (*d*) K. Sato, Y. Itoh and T. Aida, *Chem. Sci.*, 2014, **5**, 136–140.

10 (*a*) J. van Herrikhuyzen, A. Syamakumari, A. P. H. J. Schenning and E. W. Meijer, *J. Am. Chem. Soc.*, 2004, **126**, 10021–10027; (*b*) K. Sugiyasu, S. Kawano, N. Fujita and S. Shinkai, *Chem. Mater.*, 2008, **20**, 2863–2865; (*c*) A. Das and S. Ghosh, *Chem. Commun.*, 2011, **47**, 8922–8924; (*d*) S. Prasanthkumar, S. Ghosh, V. C. Nair, A. Saeki, S. Seki and A. Ajayaghosh, *Angew. Chem., Int. Ed.*, 2015, **54**, 946–950; (*e*) B. Narayan, K. K. Bejagam, S. Balasubramanian and S. J. George, *Angew. Chem., Int. Ed.*, 2015, 13245–13249.

11 (*a*) M. Kumar, K. Venkata Rao and S. J. George, *Phys. Chem. Chem. Phys.*, 2014, **16**, 1300–1313; (*b*) A. Das and S. Ghosh, *Angew. Chem., Int. Ed.*, 2014, **53**, 2038–2054.

12 (*a*) T. Aida, E. W. Meijer and S. I. Stupp, *Science*, 2012, **335**, 813–817; (*b*) L. Maggini and D. Bonifazi, *Chem. Soc. Rev.*, 2012, **41**, 211–241; (*c*) C. Kulkarni, S. Balasubramanian and S. J. George, *ChemPhysChem*, 2013, **14**, 661–673; (*d*) R. D. Mukhopadhyay and A. Ajayaghosh, *Science*, 2015, **349**, 241–242.

13 For interfacial charge transfer in co-assembly, see: (*a*) L. Zang, *Acc. Chem. Res.*, 2015, **48**, 2705–2714; (*b*) J. López-Andarias, M. J. Rodriguez, C. Atienza, J. L. López, T. Mikie, S. Casado, S. Seki, J. L. Carrascosa and N. Martín, *J. Am. Chem. Soc.*, 2015, **137**, 893–897.

14 (*a*) Z. Chen, A. Lohr, C. R. Saha-Möller and F. Würthner, *Chem. Soc. Rev.*, 2009, **38**, 564–584; (*b*) T. F. A. de Greef, M. M. J. Smulders, M. Wolffs, A. P. H. J. Schenning, R. P. Sijbesma and E. W. Meijer, *Chem. Rev.*, 2009, **109**, 5687–5754; (*c*) M. M. J. Smulders, M. M. L. Nieuwenhuizen, T. F. A. de Greef, P. van der Schoot, A. P. H. J. Schenning and E. W. Meijer, *Chem. –Eur. J.*, 2010, **16**, 362–367.

15 (*a*) M. M. J. Smulders, A. P. H. J. Schenning and E. W. Meijer, *J. Am. Chem. Soc.*, 2008, **130**, 606–611; (*b*) S. Cantekin, T. F. A. de Greef and A. R. A. Palmans, *Chem. Soc. Rev.*, 2012, **41**, 6125–6137; (*c*) B. Narayan, C. Kulkarni and S. J. George, *J. Mater. Chem. C*, 2013, **1**, 626–629.

16 (*a*) J. van Herrikhuyzen, P. Jonkheijm, A. P. H. J. Schenning and E. W. Meijer, *Org. Biomol. Chem.*, 2006, **4**, 1539–1545; (*b*) I. A. W. Filot, A. R. A. Palmans, P. A. J. Hilbers, R. A. van Santen, E. A. Pidko and T. F. A. de Greef, *J. Phys. Chem. B*, 2010, **114**, 13667–13674.

17 (*a*) P. A. Korevaar, T. F. A. de Greef and E. W. Meijer, *Chem. Mater.*, 2014, **26**, 576−586; (*b*) C. Rest, R. Kandanelli and G. Fernández, *Chem. Soc. Rev.*, 2015, **44**, 2543–2572.

18 (*a*) F. García and L. Sánchez, *J. Am. Chem. Soc.*, 2012, **134**, 734–742; (*b*) U. Mayerhöffer and F. Würthner, *Chem. Sci.*, 2012, **3**, 1215–1220; (*c*) J. M. Malicka, A. Sandeep, F. Monti,

E. Bandini, M. Gazzano, C. Ranjith, V. K. Praveen, A. Ajayaghosh and N. Armaroli, *Chem. –Eur. J.*, 2013, **19**, 12991–13001; (*d*) C. Kulkarni, K. K. Bejagam, S. P. Senanayak, K. S. Narayan, S. Balasubramanian and S. J. George, *J. Am. Chem. Soc.*, 2015, **137**, 3924–3932.

19 Nucleation-elongation model is proposed for PBI dyes linked to *tris*(dodecyloxy)benzamide with ethyl, propyl and pentyl spacer groups. This study demonstrates the importance of alkyl spacer length on determining self-assembly pathways of H-bonded PBI dyes. For details, see: (*a*) S. Ogi, V. Stepanenko, K. Sugiyasu, M. Takeuchi and F. Würthner, *J. Am. Chem. Soc.*, 2015, **137**, 3300–3307; (*b*) S. Ogi, V. Stepanenko, J. Thein and F. Würthner, *J. Am. Chem. Soc.*, 2016, **138**, 670–678.

20 (*a*) M. P. Lightfoot, F. S. Mair, R. G. Pritchard, and J. E. Warren, *Chem. Commun.* 1999, 1945–1946; (*b*) Y. Yasuda, E. Iishi, H. Inada, and Y. Shirota, *Chem. Lett*. 1996, 575–576; (*c*) P. J. M. Stals, J. C. Everts, R. de Bruijn, I. A. W. Filot, M. M. J. Smulders, R. Martín-Rapún, E. A. Pidko, T. F. A. de Greef, A. R. A. Palmans and E. W. Meijer, *Chem. –Eur. J.*, 2010, **16**, 810–821.

21 B. Rybtchinski, L. E. Sinks, and M. R. Wasielewski, *J. Phys. Chem. A* 2004, **108**, 7497–7505.

22 (*a*) Y. Che and L. Zang, *Chem. Commun.*, 2009, 5106–5108; (*b*) B.-P. Jiang, D.-S. Guo and Y. Liu, *J. Org. Chem.*, 2010, **75**, 7258–7264.

Table of contents

Supercoiled fibres of self-sorted donor-acceptor assembly allow the sensing of nitroaromatics and aromatic amines by a “turn-off/turn-on” mechanism is reported.